CALIBRATION OF DISCRETE ELEMENT PARAMETER OF SOIL IN HIGH-SPEED TILLAGE
/
高速耕作条件下土壤离散元参数标定

Shaochuan LI, Peisong DIAO*, Yongli ZHAO, Hequan MIAO, Xianghao LI, Hongda ZHAO
Shandong University of Technology, Collage of Agricultural Engineering and Food Science, ZiBo, China
*Tel: +86 13864306142 *) Corresponding author E-mail: dps2003@163.com*
DOI: https://doi.org/10.35633/inmateh-71-21

Keywords: *DEM, calibration of soil contact parameter, high-speed tillage, soil dynamic characteristic*

ABSTRACT
For the problem of lacking reliable values of soil parameters required for dynamic simulation analysis of soil under high-speed tillage, no-tillage soil was taken as the research object and its parameters were calibrated using the discrete element method in this study. The Edinburgh Elasto-Plastic Adhesion (EEPA) model was determined as the soil contact model by obtaining the loading force-deformation relationship through uniaxial sealing compression tests. The regression equation was established using Plackett-Burman test and quadratic orthogonal rotation test, and the interaction effects were analyzed. The measured values of the pile angle and strain were obtained through the pile angle test and the uniaxial seal compression test, and the optimal solution was carried out. Further, the simulated values and the measured values under the optimal parameters were compared and verified, the result showed that the error values were all less than 1%. Finally, the soil model was used for high-speed tillage simulation analysis, and the obtained soil particle displacement and groove width were compared with the measured values. It was found that the ditch width error value was 3.04% and the soil displacement was basically the same. This study proved that the contact model parameters were relatively reliable, which could provide theoretical reference for the dynamic characteristics of soil during high-speed cultivation of no-tillage soil.

摘要
针对进行高速耕作土壤动态仿真分析时所需土壤参数缺乏可靠性数值的问题，本研究以免耕土壤为研究对象，采用离散元方法对免耕土壤进行参数标定。通过单轴密封压缩试验获取加载力-变形量的关系确定 Edinburgh Elasto-Plastic Adhesion（EEPA）模型为土壤接触模型；利用 Plackett-Burman 试验和二次正交旋转试验建立回归方程，并进行交互效应的分析；通过堆积角试验和单轴密封压缩试验获取堆积角和应变的实测值并进行最优求解，将最优参数下的仿真值和实测值进行对比验证，发现误差值均小于 1%。最后以该土壤模型进行高速耕作仿真分析，将获取的土壤颗粒位移量和沟槽宽度与实测值进行对比，发现沟槽宽度误差值为 3.04%，土壤位移量基本一致。研究证明了接触模型参数较为可靠，可为免耕土壤高速耕作过程中土壤的动态特性提供理论参考。

INTRODUCTION

No-till operation can improve soil structure. However, no-till operation for a long time would cause soil compacted and show complex motion laws because of combined action of pressure, shear, and pull in soil-implement interaction (*Rusu, 2014; Cao et al., 2021; Bahrami, Naderi-Boldaji & Ghanbarian, 2020*).

The discrete element method has great advantages in revealing the soil movement characteristics in the process of agricultural machinery operation, which can not only simulate, but also predict the soil movement during the tillage process. Moreover, calibrating soil parameters in a DEM simulation is referential (*Fu & Chen, 2023; Dong, Zheng & Jia, 2022; Jan et al., 2019; Wang, Song & Zhou, 2022*). *Gao, Shang & Xu, (2022),* selected Hertz-Mindlin with JKR Cohesion model to calibrate straw-soil mixing model parameters, which provided reference and theoretical basis for studying key components of implement contacting soil in Huang Huai marine double cropping area. *Adajar et al., (2021),* used the discrete element method to calibrate five crop residues parameters and simulate interactions with soil, which proved the reliability of the discrete element method to simulate interactions. *Zhang et al., (2017),* used discrete element method consistent with soil particles characteristics to calibrate sand particles, and the dynamic behavior, velocity field, and force field of soil particles were studied based on discrete element method.

Chen et al., *(2013),* established soil particles with bonding effect using discrete element method to show soil cohesion, which could better predict soil disturbance characteristics, and calibrate the particle stiffness of different soils. *Milkevych et al., (2018),* used discrete element method to simulate tillage experiment, comparing particle displacement and soil disturbance index, and concluded that the discrete element model could accurately predict soil movement in the soil-tool interaction process under certain restrictive conditions. Discrete element method is a common way of studying soil flow in the soil-tool interaction process. *Qi & Chen, (2019),* established discrete element model to simulate soil flow process exploring soil particles flow characteristics and obtaining the sequential flow state of soil, which showed four distinctive stages: consolidating, releasing, settling, and static stages. *Fielke, Ucgul & Saunders, (2013),* established a soil discrete element model with plasticity, cohesion and adhesion according to the study of soil flow dynamic effect, which was verified by Angle of Repose, and the model effectiveness was proved through farming experiment further.

In this study, no-tillage soil model was constructed by discrete element method to study the soil motion laws and the soil particles motion characteristics in high-speed cultivation. The Elasto-Plastic model (EEPA) in EDEM software was used as the soil contact model (*Thakur, 2014*). Additionally, the repose angle and soil strain simulation test was carried out to verify the accuracy and effectiveness of soil discrete element model.

MATERIALS AND METHODS

Determination of soil basic parameters

Sandy loam soil samples (soil humidity 14.29%, volume 2×10^{-4} m^3) were collected at a depth of 10 cm using a ring knife according to the method reported by *Chen et al. (2013)*, as shown in Figure 1. The weight of soil measured using an electronic balance, and the soil wet density 1251 kg/m^3 through multiple measurements. The soil particle size was analyzed according to the particle size screening test (Figure 2) and the result showed that the soil particle size was > 4 mm 35.46%, < 4 mm 64.54%. The shape of the soil particles is represented as a single sphere to improve simulation efficiency and fit the soil shape extremely, the particles size larger than 5 mm are set to 5 mm while particles size smaller than 5 mm are set to 3 mm.

Fig. 1 - Ring knife test

Fig. 2 - Soil particle size screening test

Angle of repose and uniaxial seal compression test

Uniaxial sealing compression test is carried out on the soil to show the compaction state of no-till soil, which can better present the visco-plastic state and elastic-plastic of soil before and after compaction (*Le, Zhang & Liu, 2013; Bahrami, Naderi-Boldaji & Ghanbarian, 2020*), which is carried out at the rates of 8 mm/s, 32 mm/s and 50 mm/s respectively through a steel cylinder with a height of 200 mm and an inner diameter of 80 mm as shown in Figure 3.

Angle of repose (AOR) can directly reflect the soil mobility, which plays an important role in clarifying soil-implement interaction relationship in high-speed tillage (*Lajeunesse, Mangeney-Castelnau & Vilotte, 2004*). Therefore, a funnel with a height of 205 mm, lower diameter of 25 mm, and upper diameter of 240 mm is selected to be fixed on the iron frame, and the spacing between the funnel outlet and the plate is 95 mm (Figure 4). The funnel outlet should be opened to allow the soil to flow out naturally after the test soil poured into the funnel completely. Before that, the funnel outlet is blocked during experiment. The value of AOR is the average value after 5 measurements by protractor from different directions after the entire soil flows out and becomes static.

Fig. 3 - Uniaxial sealing compression test

Fig. 4 - Angle of repose test

The Plackett-Burman design screening test is applied to select the model parameters with influence on the test indexes significantly to avoid too many factors or some unvalued factors. The axial strain and AOR are taken as the response values in the later optimization test to study the fluidity and visco-plasticity of no-till soil in high-speed process.

Soil particle contact model

The soil presented a free and discrete state naturally, however, the action of external forces changed the original soil structure due to the fact that soil particles bond and aggregate. The relationship between deformation and axial loading force is the same basically under different loading speeds as shown in Figure 5a. It is found that the EEPA soil particle contact model combining viscosity, elasticity and plasticity has similar mechanical properties compared with the loading process of soil uniaxial seal compression test (Figure 5b), which is consistent with the description of *Thakur et al., (2014)*. Therefore, the EEPA soil particle contact model is selected as the soil particle contact model of discrete element simulation. Notably, the normal contact force and displacement become linear when n=1.

The axial strain ε_n of the consolidated sample after the test is used to characterize the soil plasticity (*Xie, Wu & Wang, 2020*). ε_n is defined as follows (Equation 2):

$$\varepsilon_n = \frac{h_0 - h_1}{h_0} \tag{1}$$

where: h_0 - Initial height of soil sample in uniaxial seal compression test, [m]; h_1 - Final height of soil sample in uniaxial seal compression test, [m]. Therefore, the pressure plate is loaded at a constant rate selecting loading rate of 32 mm/s to save test time, and unloaded at the same rate when the axial pressure reaches 300 N. The height before loading is h_0, and the height after unloading is h_1.

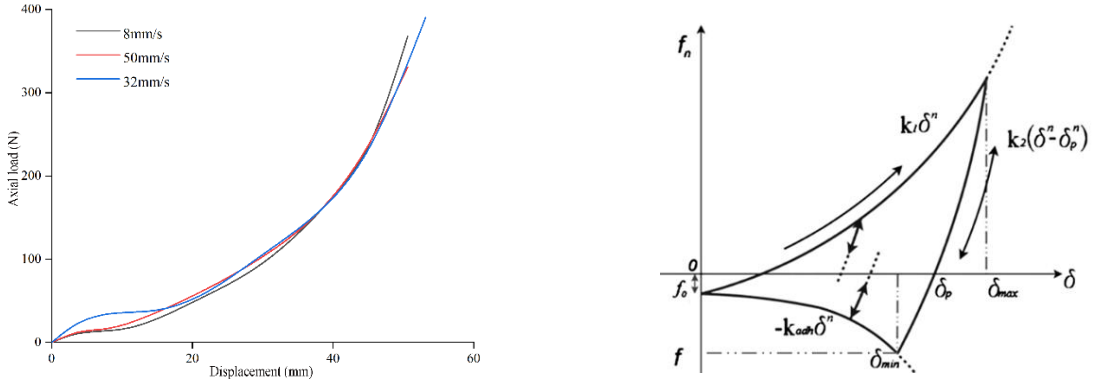

(a) (b)

Fig. 5- (a) Axial load-displacement relationship (b) EEPA normal elastic force-normal overlap relationship

Plackett-Burman test

The EEPA contact model has 7 parameters, including collision recovery coefficient, static friction coefficient, dynamic friction coefficient, constant pulling force, surface energy, contact plastic deformation, loading branch index, bonding branch index, and tangential stiffness factor. Soil model is established according to the above parameters, and the test for calibration parameter influencing on soil AOR and axial strain is

carried out. According to the simulation settings, the impact recovery coefficient, static friction coefficient, dynamic friction coefficient, constant pull-out force, surface energy, contact plastic deformation, loading branch index, bonding branch index and tangential stiffness factor are selected as the influencing factors, and AOR and axial stress are taken as the response values.

In order to reduce the number of influential factors and calibration difficulty, the above test factors are selected preliminarily. The constant pull-out force is unconsidered in this study due to the constant existence among the soil particles. The loading fraction index is selected from 1 or 1.5 in EDEM software, and 1.5 is selected according to literature finally (*Xie, Wu & Wang, 2020*). Therefore, the test factors are set as collision recovery coefficient, static friction coefficient, dynamic friction coefficient, surface energy, contact plastic deformation, bond branch index and tangential stiffness factor. Then, the appropriate level for each factor is determined, combining with the parameter selection range of references, as shown in Table 1. Relevant parameters are set as follows: soil intrinsic parameter Poisson's ratio 0.38, shear modulus 1.3×10^6 Pa. Cylinder and funnel are made of stainless steel. The Poisson's ratio, density, and shear modulus is 0.3, 7850 kg/m^3, 7×10^{10} Pa respectively (*Barr et al., 2019; Tagar et al., 2014; Mohajeri & Rhee, 2021*). The Plackett-Burman screening test is designed as shown in Table 1. A center point is used to estimate the random error of the test, including 13 sets of tests in total.

Table 1 Experimental factors and levels

Parameter	Factor	Level	
		-1	1
M_1	Collision recovery coefficient e	0.2	0.6
M_2	Static friction coefficient u_s	0.3	0.8
M_3	Dynamic friction coefficient u_r	0.1	0.6
M_4	Surface energy $\triangle\gamma$ (J/m^2)	4	20
M_5	Contact plastic deformation λ_p	0.2	0.7
M_6	Bonding branch index X	1	2.5
M_7	Tangential stiffness factor K_{tm}	0.25	0.9

RESULTS

The results of Plackett-Burman test (Table 2) are analyzed to test the significance of each factor's influence on soil characteristics, and the results of variance analysis are shown in Table 3. The significance level of 0.05 is compared with the *P*-values of each factor. According to the variance analysis of AOR, the *P*-value of the regression model is 0.0245 < 0.05, indicating that the fitting model is significant. The *P* values of e and u_s are both less than 0.05, which confirms the influence of e and u_s on the AOR is significant. The *P* value of λ_P is less than 0.01, which indicates the influence of λ_P on the AOR is extremely significant. The *P* value of K_{tm} is less than 0.05, confirming the influence of K_{tm} on axial strain is significant, while the *P* value of $\triangle\gamma$ is less than 0.01, so the influence of $\triangle\gamma$ on axial strain is extremely significant. In summary, the contact plastic deformation ratio λ_P and surface energy $\triangle\gamma$ are the main factors affecting soil properties.

Table 2

Plackett-Burman test design and results

No.	Level								AOR / °	Axial strain
	M_1	M_2	M_3	M_4	M_5	M_6	M_7	M_8		
1	1	1	-1	1	1	1	-1	-1	36.33	36.03
2	-1	1	1	-1	1	1	1	-1	45.01	25.51
3	1	-1	1	1	-1	1	1	1	21.66	37.76
4	-1	1	-1	1	1	-1	1	1	41.99	44.84
5	-1	-1	1	-1	1	1	-1	1	34.65	5.37
6	-1	-1	-1	1	-1	1	1	-1	26.04	34.23
7	1	-1	-1	-1	1	-1	1	1	32.01	29.41
8	1	1	-1	-1	-1	1	-1	1	28.74	11.67
9	1	1	1	-1	-1	-1	1	-1	23.21	6.8
10	-1	1	1	1	-1	-1	-1	1	26.7	17.54
11	1	-1	1	1	1	-1	-1	-1	28.46	26.67
12	-1	-1	-1	-1	-1	-1	-1	-1	25.22	3.75
13	0	0	0	0	0	0	0	0	38.49	41.84

Table 3

Plackett-Burman test variance analysis

Index	Variance source	Sum of squares	Df	Mean square	F	P
AOR	model	580.69	8	72.59	14.74	0.0245
	e	71.05	1	71.05	14.42	0.0320
	u_s	95.99	1	95.99	19.49	0.0216
	u_r	9.43	1	9.43	1.92	0.2604
	$\triangle\gamma$	4.89	1	4.89	0.9926	0.3925
	λ_P	372.74	1	372.74	75.67	0.0032
	X	18.35	1	18.35	3.73	0.1491
	K_{tm}	8.04	1	8.04	1.63	0.2914
	Residual error	14.78	3	4.93		
	Sum total	649.56	12			
Axial strain	model	2072.50	8	259.06	9.71	0.0440
	e	24.37	1	24.37	0.9135	0.4097
	u_s	2.25	1	2.25	0.0845	0.7903
	u_r	135.21	1	135.21	5.07	0.1098
	$\triangle\gamma$	1093.67	1	1093.67	41.00	0.0077
	λ_P	262.08	1	262.08	9.83	0.0519
	X	38.74	1	38.74	1.45	0.3146
	K_{tm}	500.78	1	500.78	18.77	0.0227
	Residual error	80.02	3	26.67		
	Sum total	2469.87	12			

Orthogonal rotation combination experiment design

Quadratic orthogonal rotation combination test is designed based on the range of Plackett-Burman to obtain the values of λ_P and $\triangle\gamma$ corresponding to the measured values. The test level coding table is shown in Table 4, and the design and results of the test are shown in Table 5. In order to ensure the test effect, the middle values of Plackett-Burman test are taken for factors having little influence on soil characteristics: e=0.4 , u_s=0.55, u_r=0.35, X=1.75, K_{tm}=0.575.

Table 4

Horizontal code table

Level	$\triangle\gamma$	λ_p
1.414	20	0.7
1	16	0.575
0	12	0.45
-1	8	0.325
-1.414	4	0.2

Variance analysis is performed on the obtained AOR and axial strain. The *P* value of the fitting multiple regression model for AOR and axial strain is 0.0021 ($P < 0.01$), 0.0014 ($P < 0.01$) as shown in Table 6, confirming that the models fitted by each index are extremely significant. The determination coefficients of AOR fitting model are $R_1^2 = 0.901$, $R_{adj1}^2 = 0.83$, and the accuracy of central composite test is greater than 4. The determination coefficients of axial strain fitting model are $R_2^2 = 0.913$, $R_{adj2}^2 = 0.85$, and the accuracy of central composite test is greater than 4. Therefore, the results indicate that the fitting model is better and good predictive.

Table 5

Experimental scheme and results

Number	$\triangle\gamma$	λ_P	AOR	Axial strain
1	-1	-1	37.26	30.43
2	1	-1	32.72	11.29
3	-1	1	36.08	28.78
4	1	1	30.91	32.39

Number	$\triangle\gamma$	λ_P	AOR	Axial strain
5	-1.414	0	38.59	31.81
6	1.414	0	20.49	26.25
7	0	-1.414	29.64	9.84
8	0	1.414	37.93	19.05
9	0	0	20.45	21.13
10	0	0	20.21	23.94
11	0	0	20.84	21.13
12	0	0	20.23	22.53
13	0	0	20.89	23.94

Table 6

Analysis of variance

index	Variance source	Sum of squares	D_f	Mean square	F	P
AOR	model	658.76	5	131.75	12.75	0.0021
	$\triangle\gamma$	155.83	1	155.83	15.08	0.0060
	λ_P	9.53	1	9.53	0.9225	0.3688
	$\triangle\gamma\lambda_P$	0.0992	1	0.0992	0.0096	0.9247
	$\triangle\gamma^2$	184.72	1	184.72	17.87	0.0039
	${\lambda_P}^2$	368.23	1	368.23	35.63	0.0006
	Residual error	72.35	7	10.34		
	Sum total	731.11	12			
Axial strain	model	546.75	5	109.35	14.67	0.0014
	$\triangle\gamma$	68.40	1	68.40	9.18	0.0191
	λ_p	131.83	1	131.83	17.69	0.0040
	$\triangle\gamma\lambda_p$	129.39	1	129.39	17.36	0.0042
	$\triangle\gamma^2$	125.31	1	125.31	16.82	0.0046
	${\lambda_p}^2$	64.64	1	64.64	8.67	0.0216
	Residual error	52.16	7	7.45		
	Sum total	598.91	12			

According to the experimental results and further analysis, the *P* values of the regression terms $\triangle\gamma$, $\triangle\gamma^2$ and ${\lambda_p}^2$ are all less than 0.01, indicating that they have significant influence on AOR. The significant influence degree of all items on the axial strain ranges from large to small as λ_p, $\triangle\gamma\lambda_p$, $\triangle\gamma^2$, $\triangle\gamma$, ${\lambda_p}^2$. The *P* values of the regression terms λ_p, $\triangle\gamma\lambda_p$ and $\triangle\gamma^2$ are less than 0.01, indicating that the influence on the axial strain is extremely significant, the P values of the regression terms $\triangle\gamma$ sum and ${\lambda_p}^2$ are less than 0.05, confirming that the influence on the axial strain is significant. The Design-Expert 12 software is used to refit to obtain the quadratic regression equation after removing nonsignificant items. The AOR and axial strain are represented by A and ε_n as shown in Equation 2, respectively:

$$\begin{cases} A = 20.52 - 4.41\Delta\gamma + 1.09\lambda_p + 5.15\Delta\gamma^2 + 7.28{\lambda_p}^2 \\ \varepsilon_n = 22.53 - 2.92\Delta\gamma + 4.06\lambda_p + 5.69\Delta\gamma\lambda_p + 4.24\Delta\gamma^2 - 3.05{\lambda_p}^2 \end{cases} \quad (2)$$

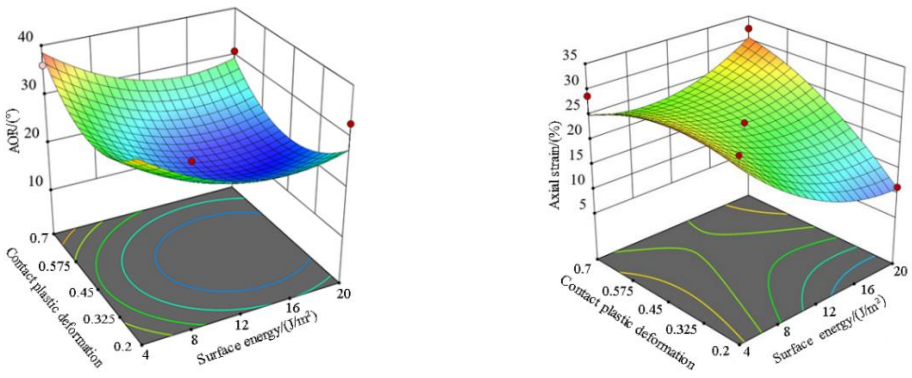

(a) (b)

Fig. 6 - Effect of interaction on AOR and axial strain

The interaction of the contact plastic deformation ratio λ_p and surface energy $\triangle\gamma$ on AOR and axial strain is analyzed by the response surface, as shown in Figure 6. The response surface presents obvious slope (Figure 6a), indicating that the interaction effect of λ_p-$\triangle\gamma$ has a significant influence on the AOR, and the contours show large curvature, The response surface presents obvious slope (Figure 6b), indicating that the interaction effect of λ_p-$\triangle\gamma$ has a significant influence on the axial strain, and the contours show large curvature change.

The optimization function of Design-Expert 12 software is used to optimize the parameters, and the regression model is optimized by taking the measured stacking angle and axial strain as the target values. The actual test value shows that the angle of repose is 37.74° and the axial strain is 28.12%. At the same time, the importance of the two indexes is set. Setting the stacking angle as "+++" and axial strain as "++++".

The surface energy of soil particles is 7.32 J/m^2 and the contact plastic deformation ratio is 0.543. The parameters of the EEPA contact model are set as optimal values, and other parameters are set as intermediate levels, three simulation tests are carried out for AOR and axial strain respectively in EDEM. The results of AOR are 38.1°, 37.66° and 37.88°, and the errors with the measured values are all less than 0.95%.

The results of axial strain are 27.84%, 28.39%, 28.04%, and the errors of the measured values are all less than 1%. Further, the strain of the soil is calculated using the above formula, and the relation curve of axial stress-strain is shown in Figure 7. Based on the above analysis, it can be seen that the value simulation can match the actual value.

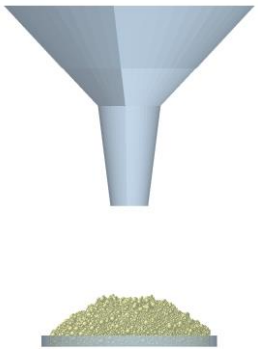

(a)

Fig. 7-(a) Angle of repose simulation test

(b)

Fig. 7- (b) Uniaxial seal compression simulation test

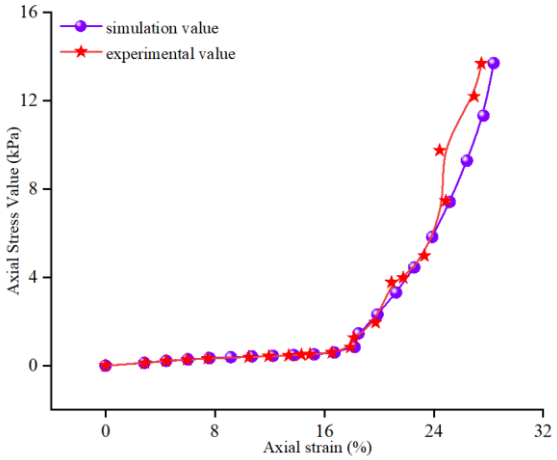

(c)

Fig. 7- (c) Axial stress-strain curve

Validation test

This experiment combined the real test and the discrete element test to further verify whether the optimized parameters of the discrete element soil model can truly reflect the soil mechanical properties in high-speed operation. The soil displacement values and ditch widths in simulation experimenting under different test speeds values are analyzed to verify the accuracy of the parameters using error indicators.

(a)

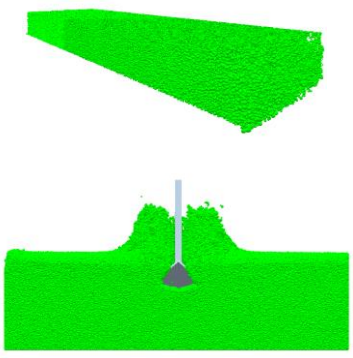

(b)

Fig. 8 - Field tillage test

Field tillage test is carried out in the soil sampling area to obtain the measured values. The tool, as shown in Figure 9a, is used to limit the maximum tillage depth to 60 mm. During the test, the tool is allowed to pass through the working area at a constant speed of 12 km/h, 13 km/h, 14 km/h, and the working distance is 4 m. The soil bin with length× width × height of 4000 mm×300 mm×200 mm is established by using EDEM software, and the soil bin is quickly generated by means of particle bed according to the calibrated discrete element parameters. The 3D model of tool, embedding basically with the real object, is imported into the EDEM software after the formation of the soil bin. The tillage depth is set to 60 mm and the speed is 12 km/h, 13 km/h and 14km/h, as shown in Figure 9b.

v=12km/h v=13km/h v=14km/h

Fig.9 - Measure ditch width

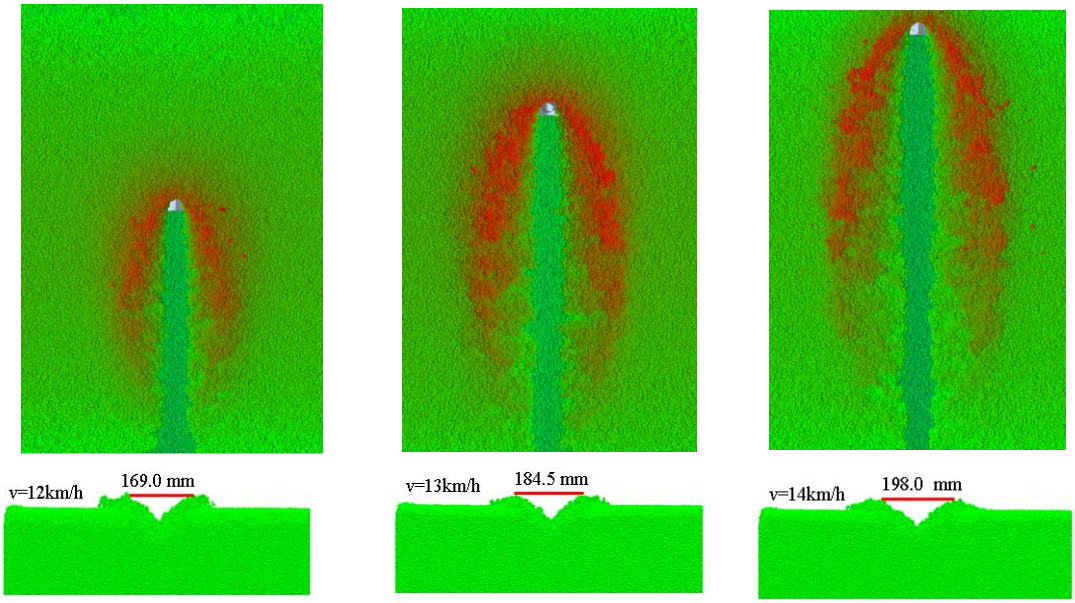

Fig. 10 - Ditch width simulation value

The measurement of ditch width, soil compaction and tillage will produce soil disturbance, affecting the physical properties of soil. The amount of soil disturbance can be represented by the ditch width. The virtual soil bin is tillage at different speeds to obtain the disturbance characteristics of the soil in the process of high-speed tillage. Five points are randomly selected to measure the ditch width after each tillage is completed, and the average value of 5 points is taken as the ditch width value, as shown in Figure 9. The field test results show that the ditch widths are 164.0 mm, 182.0 mm and 201.0 mm under the cultivation speed of 12 km/h, 13 km/h and 14 km/h respectively.

After the simulation of the tillage process is completed, the soil particles continue to calculate a certain time step, and the tool function of EDEM software is used to measure the ditch width under high-speed tillage, as shown in Figure 10.

The measured ditch widths at 12 km/h, 13 km/h, and 14 km/h are 169.0 mm, 184.5 mm, and 198.0 mm respectively. The error between experimental value and the simulation value is less than 3.04%, confirming that the simulation value is reliable. Soil particles obtain greater kinetic energy when the tool operates with larger speed, leading to the soil particles in contact with implement pressing on adjacent soil particles with a larger force, so a larger disturbance area and larger width of the ditch will be generated in the meantime.

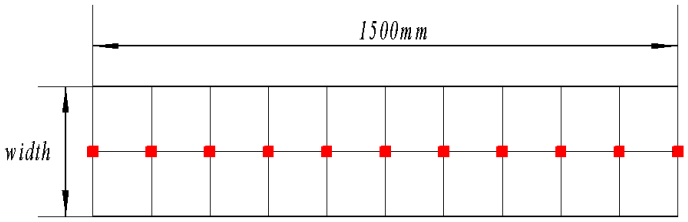

Fig. 11 - Schematic representation of Tracer distribution

Soil particle displacement can show the fluidity of soil-tool interaction, which is measured by tracer tracking method. The specific implementation plan is shown in Figure 11. An area with a working length of 1500 mm and a working width of 450 mm is selected in the middle of the working distance. A tracer is set every 150 mm, a total of 10 tracers being set, having the labels 1, 2, 3 to 10. The tillage direction is X direction, the width direction is Y direction, and the tillage depth direction is Z direction. After the tillage is completed, the displacement change of the tracer in the three directions is measured and the measurement results are shown in Figure 12.

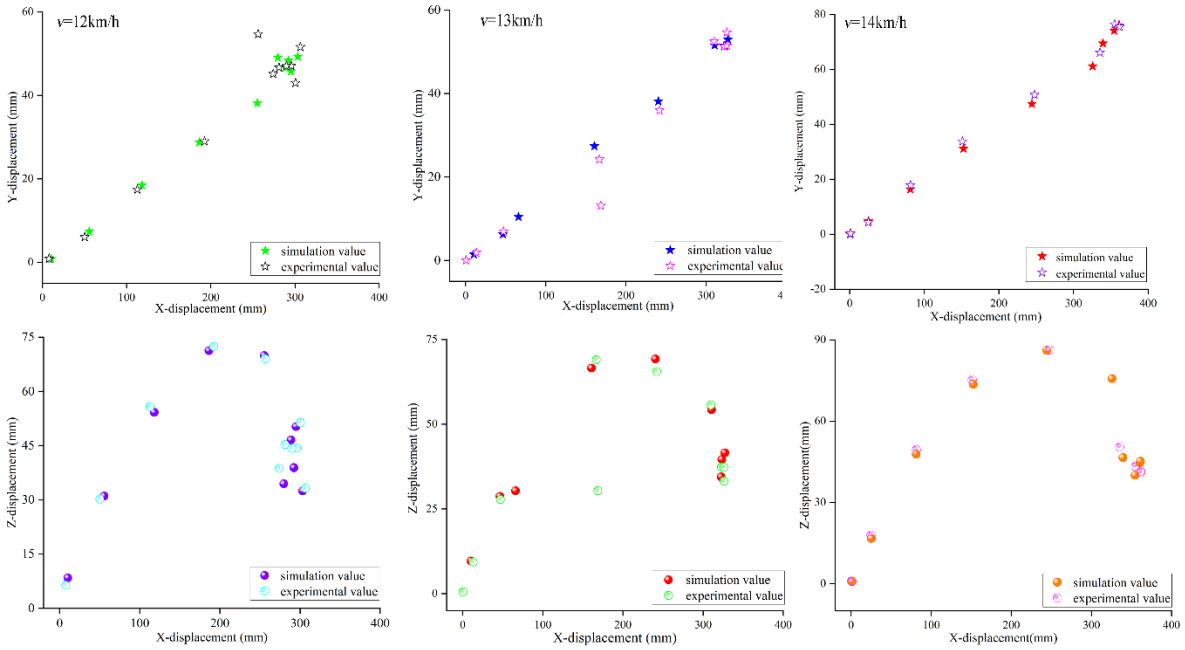

Fig. 12 - Soil displacement

The post-processing function in EDEM software is used to select ten regions and number them as 1-10 successively according to the actual tracer placement method. The displacement of particles in each region in three directions is obtained to ensure that the volume of the regions is consistent with the volume of the tracer, and the same number of soil particles in each region. It can be seen from Figure 12 that the simulation results are basically consistent with the experimental values, indicating that the model can better predict the soil displacement in high-speed cultivation process.

In order to further obtain the information of the soil-tool interaction, soil particles in the tillage area are selected as the research object of displacement. The value of the particle displacement in the X-axis direction, Y-axis direction and Z-axis direction are obtained. The time-displacement curves of particles at different speeds are obtained through data processing software, as shown in Figure 13.

It can be seen the soil particles have a large displacement in the three directions when the speed is 14 km/h. The difference in the change rate in the Z direction is significant, while the change rate in the X and Y directions is relatively small.

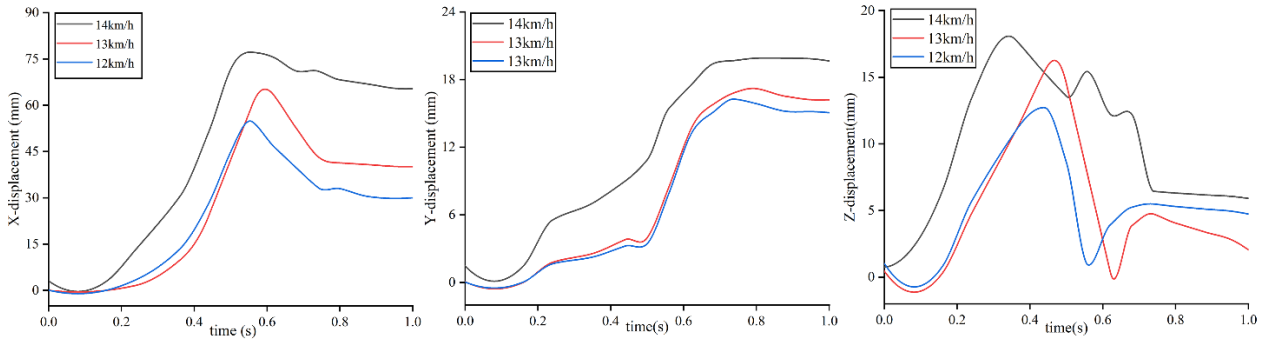

Fig. 13 - Soil average displacement in cultivation area

CONCLUSIONS

(1) The no-till soil was taken as the research object and the Edinburgh Elasto-Plastic Adhesion (EEPA) was chosen as contact model to calibrate the soil parameters using the discrete element method, which lays the foundation for the research on the soil dynamics properties and soil-tool interactions in the process of high-speed tillage.

(2) Plackett-Burman method was used to screen out that the plastic variable ratio λ_P and surface energy $\Delta\gamma$ had significant effects on AOR and soil strain. Quadratic orthogonal regression test was conducted according to the test result of Plackett-Burman method, the regression equation was established and the interaction effects of the factors were analyzed. The AOR test and uniaxial seal compression test were used to obtain the measured values of AOR and soil strain for optimal solution. After optimization, the plastic variation ratio λ_P is 0.543, and the surface energy $\Delta\gamma$ is 7.32 J/m^2.

(3) The optimized parameters were used for simulation tests. The error values were both less than 1% by comparing AOR and strain of simulation and experiment, and the stress-strain curves of simulation were basically consistent with the experiment, proving the reliability of the model. The error between the simulated value and the measured value of the ditch width was less than 3.04% after comparison, and the simulated value and the measured value of the soil displacement are basically the same. Therefore, the model predicts the soil dynamic characteristics in high-speed tillage.

ACKNOWLEDGEMENT

This paper was Supported by “the National Key Research and Development Program of China” (2021YFD2000401).

REFERENCES

[1] Adajar J., Alfaro M., Chen Y., Zeng Z., (2021), Calibration of discrete element parameters of crop residues and their interfaces with soil. *Computers and Electronics in Agriculture*, Vol.188, pp.106349.

[2] Bahrami M., Naderi-Boldaji M., Ghanbarian D., (2020), Dem simulation of plate sinkage in soil: calibration and experimental validation. *Soil & Tillage Research*, Vol.203, pp.104700.

[3] Barr J.B., Ucgul M., Desbiolles J., Fielke, J., (2019), Development and field evaluation of a high-speed no–till seeding system. *Soil & Tillage Research*, Vol.194, pp.104337.

[4] Cao X., Wang Q., Li H., (2021), Combined row cleaners research with side cutter and stubble clean disk of corn no-till seeder (玉米免耕播种机侧置切刀与拨茬齿盘组合清茬装置研究). *Transactions of the Chinese Society for Agricultural Machinery*, Vol.52, Issue 03, pp.36-44.

[5] Chen Y., Munkholm L.J., Nyord T., (2013), A discrete element model for soil–sweep interaction in three different soils. *Soil & Tillage Research*, Vol.126, pp.34-41.

[6] Dong X., Zheng H., Jia X., (2022), Calibration and experiments of the discrete element simulation parameters for rice bud damage. *INMATEH Agricultural Engineering*, Vol.68, Issue 03, pp.659-668. https://doi.org/10.35633/inmateh-68-65

[7] Jan D.P., Gemmina D.E., Verastegui F.R.D., Adam B., Cornelis W.M., (2019), Calibration of DEM material parameters to simulate stress-strain behaviour of unsaturated soils during uniaxial compression. *Soil & Tillage Research*, Vol.194, pp.104303.

[8] Fu M., Chen X., (2022), Parameters calibration of discrete element model for crushed corn stalks. *INMATEH Agricultural Engineering*, Vol. 69, Issue 01, pp. 399-408. https://doi.org/10.35633/inmateh-69-37

[9] Fielke J.M., Ucgul M., Saunders C., (2013), Discrete Element Modeling of Soil-Implement Interaction Considering Soil Plasticity, Cohesion and Adhesion. Kansas City, Missouri.

[10] Gao Z., Shang S., Xu N., (2022), Parameter calibration of discrete element simulation model of wheat straw-soil mixture in Huang Huai Hai production area (黄淮海产区小麦秸秆-土壤混合物的离散元仿真模型参数标定). *INMATEH Agricultural Engineering*, Vol.66, Issue 01, pp.201-210.

[11] Le V., Zhang J., Liu X., (2013), Ride comfort evaluation of vibratory roller under different soil ground (振动压路机用于不同土壤地面的平顺性评价). *Transactions of the Chinese Society of Agricultural Engineering*, Vol.29, Issue 9, pp.39-47.

[12] Lajeunesse E., Mangeney-Castelnau A., Vilotte J.P., (2004), Spreading of a granular mass on a horizontal plane. *Physics of Fluids*, Vol.16, Issue 7, pp.2371-2381.

[13] Milkevych V., Munkholm L.J., Chen Y., Nyord T., (2018), Modelling approach for soil displacement in tillage using discrete element method. *Soil & Tillage Research*, Vol.183, pp.60-71.

[14] Mohajeri M., Rhee C., (2021), Replicating cohesive and stress-history-dependent behavior of bulk solids: feasibility and definiteness in DEM calibration procedure. *Advanced Powder Technology*, Vol.32, Issue 5, pp.1532-1548.

[15] Qi L., Chen Y., (2019), Simulations of soil flow properties using the discrete element method (DEM). *Computers and Electronics in Agriculture*, Vol.157, pp.254-260

[16] Rusu T., (2014). Energy efficiency and soil conservation in conventional, minimum tillage and no-tillage. *International Soil & Water Conservation Research*, Vol.2, Issue 4, pp. 42-49.

[17] Thakur S.C., Morrissey J.P., Sun J., Chen J.F., Ooi J.Y., (2014), Micromechanical analysis of cohesive granular materials using the discrete element method with an adhesive elastoplastic contact model. *Granular Matter*, Vol.16, Issue 3, pp.383-400.

[18] Tagar A.A., Ji C., Adamowski J., Malard J., Abbasi, N.A., (2014), Finite element simulation of soil failure patterns under soil bin and field testing conditions. *Soil & Tillage Research*, Vol.145, pp.157-170.

[19] Wang W., Song J., Zhou G., (2022), Simulations and experiments of the seedbed straw and soil disturbance as affected by the strip-tillage of rowcleaner (带状耕作对种床秸秆清除率和土壤扰动的仿真与试验). *INMATEH Agricultural Engineering*, Vol.66, Issue 01, pp.49-61.

[20] Xie F., Wu Z., Wang X., (2020), Calibration of discrete element parameters of soils based on unconfined compressive strength test. *Transactions of the Chinese Society of Agricultural Engineering*, Vol.36, Issue 13, pp.39-47.

[21] Zhang R., Han D., Ji, Q., (2017), Calibration Methods of Sandy Soil Parameters in Simulation of Discrete Element Method (离散元模拟中沙土参数标定方法研究). *Transactions of the Chinese Society for Agricultural Machinery*, Vol.48, Issue 03, pp.49-56.